

## Numerical Assessment of Temperature Distribution in the Orthotropic Steel Deck and Main Truss of a Rail-cum-road Bridge

Taimur Rahman<sup>1</sup> and Dr. Pengfei Zheng<sup>2</sup>

<sup>1</sup>Master's Student, Dept. of Civil Engineering, Zhengzhou University, Zhengzhou, China.

<sup>2</sup>Dr., Dept. of Civil Engineering, Zhengzhou University, Zhengzhou, China.

Corresponding Author: Pengfei Zheng

**ABSTRACT:** Steel truss bridge with its extensive spanning capacity and higher mechanical performance, gradually becomes the preferred form of long-span bridges especially the bridge with highway and railway. Because, steel bridges are more sensitive to temperature, after bridge structures exposed to the environment for a long time, it will be affected by the periodic change of ambient temperature and solar radiation. Besides that, geographical features have a significant impact on the characteristics of temperature load. Considering these issues, this paper introduced a two-dimensional numerical finite element model to analyze the temperature distribution in steel truss bridges. Then the temperature distribution behaviors of the main steel truss frame along with the orthotropic steel highway deck of the Tianxingzhou Yangtze River Bridge in Wuhan, China are conducted thoroughly with the commercial FEM program ANSYS APDL using the introduced mathematical model considering local metrological data and geographical features. Finally, computed results of vertical thermal gradients are compared with British Standard Code BS5400 and German National Standard DIN101 to check the validity of the introduced FEA model. The study shows that, the introduced numerical finite element model is adequate to carry out the transient analysis and analyze the thermal distribution behavior of the steel bridges.

**KEYWORDS:** thermal distribution, steel truss bridge, Finite element analysis, orthotropic steel deck, temperature variation.

Date of Submission: 25-05-2020

Date of acceptance: 10-06-2020

### I. INTRODUCTION

With the development of modern bridge structure in the direction of the economy, environment coordination, and large span, more and more attention has been paid to the damage of bridge structure caused by temperature gradient effect. Therefore, in the design of the bridge structure, designers need to know the distribution characteristics of the temperature field and the magnitude of the temperature gradient to consider these factors in the design process of the bridge. With the continuous innovation and development of engineering materials, concrete materials are no longer the primary choice of bridge construction, steel structure bridges are more and more concerned by the industry. The orthotropic steel bridge deck with its unique advantages is widely used in their respective bridge structure forms. They are a very economical and easy to build due to the modern construction techniques. For the steel structure bridge, because of the good thermal conductivity and the sensitivity to temperature change, the structural temperature gradient change may not be so obvious in the steel bridge deck, although because of different radiation condition from the main truss, it may induce a large temperature variation between bridge deck and main truss, which may induce large stress between two part, so more detailed research on the temperature distribution in main truss and steel bridge deck is needed<sup>[1]</sup>.

From the beginning of the early 1960s, researchers began to study the uneven temperature distribution of concrete girders. Early in the 1960s, Zuk<sup>[2]</sup> started a study on the thermal behavior of highway bridges. From the late 1970s to early 1990, with the increasing popularity of computers and the maturity of the finite element algorithm took the study in a whole new level<sup>[3-5]</sup>. From the early 1990s the study about this topic became more

sophisticated and lots of variation about parameters, structural materials, the complex numerical analysis started to include in the study. The study about the concrete bridge, steel bridge, and steel-concrete composite bridge are still growing on to fulfill the ongoing demand in this sector and meet the challenges which are rising all over the world. At present, China is at the peak of bridge construction. Steel bridges have been widely used for their excellent mechanical properties, construction performance, and economics. The research on steel bridges is in full swing<sup>[6-11]</sup>. The design of steel bridges used by engineers is still based on the theory of the temperature field of original concrete bridges. So, Research on temperature distribution and temperature effects in steel bridges is very necessary.

The approach of this study can be divided into three parts. At first a proper finite element model is developed based on heat exchange theory and mathematic methods considering solar physics, the sectional property of the structure, thermal property of materials, and meteorological science. In the second stage, an extensive transient analysis based on the above-mentioned mathematical model is carried out under proper boundary conditions associated with the Tianxingzhou Yangtze River Bridge and publicly available local metrological data in bridge location. The temperature distribution behavior, in the summertime, of the main girders of the bridge and orthotropic bridge deck is mainly assessed in this stage of the study. Finally, the calculated thermal gradient values are compared with a few related national bridge design codes to check the validity of the finite element model used in this study. Due to the lack of detailed specifications about the thermal gradient of steel bridges in different countries national bridge design codes, only British Standard Code and German National Standard are selected to compare the thermal gradient values.

## II. THE BASIC PRINCIPLE OF TEMPERATURE DISTRIBUTION

### 2.1 HEAT TRANSFER

Heat can be transferred from one point to another in three ways: conduction in solids, convection of fluids (liquids or gases), and radiation through anything, that will allow radiation to pass.

#### i) Thermal convection

Thermal convection occurs mainly on the surface of the structure. According to Newton's Law of Cooling equation,

$$q = h(T_s - T_b) \quad (1)$$

Where;  $q$  — Heat flux density ( $W/m^2$ )

$h$  — Flow Heat transfer coefficient ( $m^2 \cdot h \cdot ^\circ C$ )

$T_s$  — The temperature of the solid surface ( $^\circ C$ )

$T_b$  — Temperature of surrounding fluids ( $^\circ C$ )

#### ii) Heat conduction

Conduction occurs when two objects at different temperatures are in contact with each other. From Fourier's law:

$$q = -\lambda \frac{\partial T}{\partial n} \quad (2)$$

Where,  $\lambda$  - Thermal conductive coefficient ( $W/m \cdot ^\circ C$ );

#### iii) Thermal radiation

Heat transfer from a body with a high temperature to a body with a lower temperature, when bodies are not in direct physical contact with each other or when they are separated in space, is thermal radiation.

By Stefan-Boltzmann equation;

$$q = \varepsilon C_0 F_{ij} (T_1^4 - T_2^4) \quad (3)$$

Where  $q$  — Heat flux density ( $W/m^2$ )

$\varepsilon$  — Radiation rate (blackness) ;

$C_0$  — Stephen a Boltzmann constant, (approx.  $5.67 \times 10^{-8} W \cdot m^{-2} \cdot K^{-4}$ )

$F_{ij}$  — The shape coefficient of a radiation surface B by radiation surface A;

$T_1$  — Absolute temperature of radiation surface A (K);

$T_2$  — Absolute temperature of radiation surface B (K);

### 2.2 FEA MODEL

To obtain the temperature effect of the bridge, the temperature load must be solved first. The performance of the temperature load on the bridge is the temperature field changing with time in the bridge. Therefore, the first problem to be solved in analyzing the temperature effect in the bridge is to solve the temperature field.

The temperature  $t$  at a point in the bridge structure can be expressed as :

$$t = f(x, y, \tau) \quad (4)$$

In this formula;  $t$  — temperature

$x, y, z$  — three-dimensional coordinates

$\tau$  — time

From the above equation, it is clear that the temperature field analysis of bridges can be divided into two categories: the steady temperature field which is related only to the coordinates, and the unsteady temperature field which is related to the change of coordinates and time. According to the relationship with the coordinate dimension, it can be divided into a one-dimensional temperature field, two-dimensional temperature field, or three-dimensional temperature field.

The temperature gradient vector of the two-dimensional temperature field can be expressed in the following formula:

$$\text{grad}t = \frac{\partial t}{\partial x} i + \frac{\partial t}{\partial y} j \quad (5)$$

Heat flux density refers to the heat passed through the unit area over a unit of time, expressed in  $q$ . Then according to equation (2) can be expressed as:

$$q = -\lambda * \text{grad}t \quad (6)$$

In this formula:  $\lambda$  — Thermal conductivity ( $\text{kJ}/(\text{hr} * \text{k} * \text{m})$ )

The spatiotemporal differential relations of physical internal temperature are derived from the law of conservation of energy and Fourier's laws, that is, the differential equations of thermal conductivity:

$$\rho c \frac{\partial t}{\partial \tau} = \text{div}(\lambda * \text{grad}t) + q_v \quad (7)$$

In the formula :  $q_v$  — Heat released per unit volume

$\lambda, c, \rho$  — Conductivity, specific heat capacity, density

If the thermal property is constant, the three-dimensional unsteady thermal conductivity equation can be written in the following:

$$\frac{\partial t}{\partial \tau} = \alpha \left( \frac{\partial^2 t}{\partial x^2} + \frac{\partial^2 t}{\partial y^2} \right) + \frac{q_v}{\rho c} \quad (8)$$

In the formula :  $\alpha$  — Called Thermal diffusion rate,  $\alpha = \frac{\lambda}{\rho c}$

If there is no internal heat source, the upper formula can be reduced to:

$$\frac{\partial t}{\partial \tau} = \alpha \left( \frac{\partial^2 t}{\partial x^2} + \frac{\partial^2 t}{\partial y^2} \right) \quad (9)$$

From the above formula, it is clear that the left and right sides of the equation accurately represent the principle of energy conservation. It mainly expresses the equation of energy change caused by the temperature change in unit time. Formula (8) and (9) can be defined as basic differential equations of thermal conductivity.

To solve the basic differential equations of thermal conductivity, the solution conditions that need to be met, include Thermophysical properties of materials, heat source conditions, geometric conditions, initial state values, and boundary conditions. There are three types of boundary conditions:

(i) The temperature limit of the study object,  
 $\tau > 0$  when,  $t_w = f(\tau)$  (10)

(ii) The heat flux density limit of the study object,  
 $\tau > 0$  when,  $-\lambda \left( \frac{\partial t}{\partial n} \right)_w = f(\tau)$  (11)

(iii) Convection heat transfer boundary condition,  
 $-\lambda \left( \frac{\partial t}{\partial n} \right)_w = h(t_w - t_f)$  (12)

Radiation heat transfer boundary condition:

$$-\lambda \left( \frac{\partial t}{\partial n} \right)_w = \sigma(t_w^4 - t_f^4) \quad (13)$$

Compound heat transfer boundary condition:

$$-\lambda \left( \frac{\partial t}{\partial n} \right)_w = h(t_w - t_f) + \sigma(t_w^4 - t_f^4) \quad (14)$$

### 2.3 FINITE ELEMENT SOLUTION TO TEMPERATURE DISTRIBUTION

Finite element method is an approximate calculation method, which has strong applicability and flexibility, can solve the analysis of the Heat conduction problem in any form <sup>[12]</sup>.

i) Separation of unit division and temperature field:

On the area  $O$ , divided into arbitrary unit area  $O^e$ , any point within the unit  $(x, y)$  of the temperature  $T$ , in the finite element method,

$$T = f(T_i, \dots, T_m) \quad (15)$$

We just need the discrete temperature  $T_1, \dots, T_m$ , to obtain any bit of temperature inside the unit from the formula T.

$$[T] = [N][T^e] \tag{16}$$

ii) A variational method for solving temperature field:

The third type of boundary condition can be considered, when the temperature variation dT considered as an arbitrary function, the variational principle of the heat conduction problem can be expressed as;  $\delta\Pi = 0$

Where,

$$\Pi(T) = \int_{\Omega} \left\{ \frac{\lambda}{2} \left[ \left( \frac{\partial T}{\partial x} \right)^2 + \left( \frac{\partial T}{\partial y} \right)^2 + \left( \frac{\partial T}{\partial z} \right)^2 \right] - q_v T + c\rho \frac{\partial T}{\partial t} T \right\} d\Omega + \int_r \left( \frac{\lambda}{2} dT^2 - dT_f T \right) ds \tag{17}$$

According to the variational principle,

$$\delta\Pi = \sum_e \delta T^e \frac{\partial \Pi^e}{\partial T^e} = 0 \tag{18}$$

Where,

$$\delta\Pi = \sum_e \delta T^e \frac{\partial \Pi^e}{\partial T^e} = \left[ \frac{\partial \Pi^e}{\partial T_1^e}, \dots, \frac{\partial \Pi^e}{\partial T_m^e} \right] = [M]^e [\dot{T}]^e + [K]^e [T]^e - [P]^e \tag{19}$$

In the previous formula,

$[P]^e$ — Unit temperature load vector,  $[P]^e = \int_{\Omega_e} q_v N^T d\Omega + \int_{\Gamma_e} \alpha T_f N^T d\Gamma$

$[M]^e$ — Unit temperature load,  $[M]^e = \int_{\Omega_e} c\rho N N^T d\Omega$

$[K]^e$ — Unit Stiffness,  $[K]^e = \int_{\Omega_e} \lambda \left( \frac{\partial N^i}{\partial x} \frac{\partial N^j}{\partial x} + \frac{\partial N^i}{\partial y} \frac{\partial N^j}{\partial y} + \frac{\partial N^i}{\partial z} \frac{\partial N^j}{\partial z} \right) d\Omega + \int_{\Gamma_e} \alpha N^T N d\Gamma$

The unit summary is:

$$\delta\Pi = \sum_e (\delta T^e M \dot{T} + \delta T^e K T^e - \delta T^e P^e) = \delta T^e (M \dot{T} + K T^e - P^e) \tag{20}$$

Where,

$[M]$ — Transient temperature stiffness matrix ;

$[K]$ — Temperature stiffness matrix ;

$[T]$ — Column vectors for unknown temperature values ;

$[P]$ — Temperature load Column vector ;

Solving the above ordinary differential equation with time as a variable, the node temperature can be obtained at any time.

### III. ANALYTICAL DATA AND FEA MODEL

#### 3.1 TIANXINGZHOU YANGTZE RIVER BRIDGE

Tianxingzhou Yangtze River Bridge consists of three planes of trusses at a span arrangement of 98+196+504+196+98 m. It is a double-deck bridge where the upper deck carries six highway lanes and the bottom deck is a railway deck with two railway tracks (design speed is over 250 km/h)<sup>[13]</sup>. Details of the bridge are shown in figure 1 and figure 2. The upper deck is an orthotropic plate except for the outermost 168m at both ends of the bridge<sup>[13]</sup>. Though it is partially a steel-concrete composite bridge, in this study the steel part is focused on. In this study, the orthotropic highway deck will consider combined with the main steel truss frame and bottom railway deck. And for orthotropic deck 30 mm thick steel plate is considered with 12 mm U-rib member.

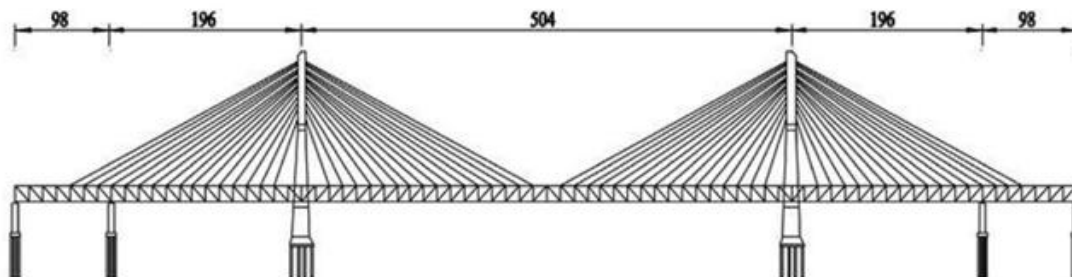


Figure 1 Elevation view of Tianxingzhou Yangtze River Bridge (unit: m)<sup>[14]</sup>

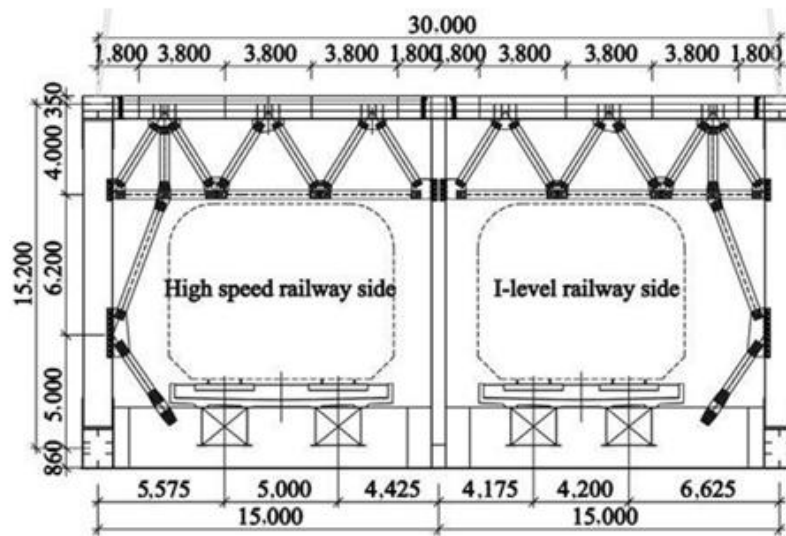


Figure 1 Typical cross section of Tianxingzhou Yangtze River Bridge (unit: mm)<sup>[14]</sup>

### 3.2 FEA MODEL

The thermal analysis of ANSYS is divided into steady-state thermal analysis and transient thermal analysis. The temperature field of the first one is independent of time, while the temperature field of the other one changes at any time. In this thesis, the transient thermal analysis method is used. In the process of solving the temperature field by ANSYS APDL, PLANE 55 is used to develop the model. PLANE 55 is adopted as a plane element, which can be used to analyze the transient analysis of two-dimensional heat conduction.

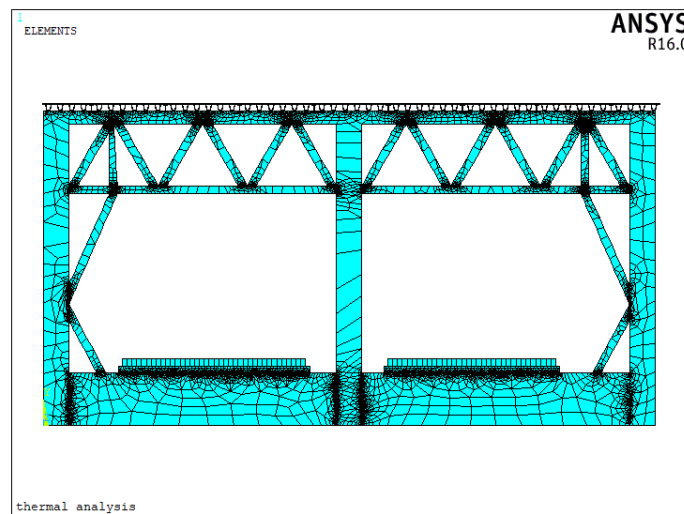


Figure 2 Bridge cross section in ANSYS with elemental meshing

There are 21848 elements and 27905 nodes in the analysis model.

### 3.3 ANALYTICAL DATA

For transient analysis hottest time in the summer of 2019, July 21 to July 26, is selected as an analysis period. The geographical location of Wuhan, China is latitude 30.6569 North, longitude 114.405 East. Daily average maximum temperature in this period is 36°C, daily average minimum temperature: 26.0 °C and the average wind speed is taken as 3m/s<sup>[15]</sup>. It is being assumed that the temperature distribution in the longitudinal direction is constant throughout the bridge.

The materials which are used in the analysis are summarized in table 1.

**Table 1:** Thermal properties of materials

Property	Concrete	Steel	Ballast	Internal air
Density [kg/m <sup>3</sup> ]	2500	7850	1910	1.29
Specific heat capacity, c [kJ/ (kg. °C)]	0.96	0.46	0.98	1
Thermal conductivity, λ [kJ/ (hr. k. m)]	10.8	216	2.24	0.0864
Emissivity	0.88	0.8	0.88	-
Absorptivity	0.65	0.75	0.6	-

**IV. TEMPERATURE DISTRIBUTION RESULTS**

The temperature distribution behavior for steel orthotropic highway deck and main steel truss frame members will be discussed. The orthotropic steel deck may experience very high temperatures in its top surface and that’s why the temperature behavior of this steel bridge deck will be focused on separately. The temperature distribution result of the 5<sup>th</sup> day is represented in figure 4. The internal air is not shown in the graphical

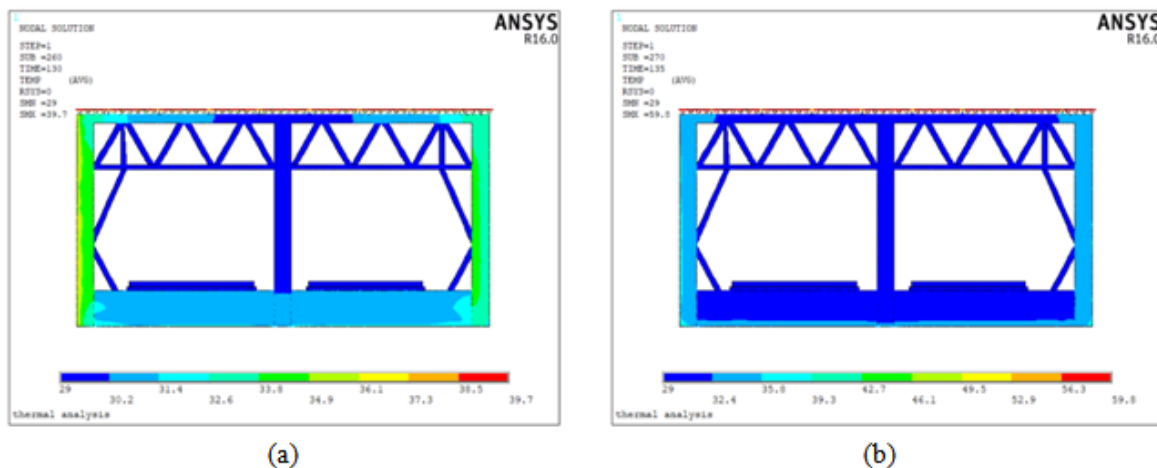


**Figure 4** Temperature distribution in the bridge (units: °C): (a) At 10 AM; (b) At 3 PM

The upper highway deck’s, steel orthotropic deck, the temperature rises very high during the day time in comparison to the rest of the members of the bridges because it is exposed to direct solar radiation, and steel is very sensitive to temperature which causes a rapid temperature increase. The maximum temperature of this surface is 59.8°C at 3PM [figure 4 (b)]. The direct solar radiation does not affect the inner members, so the temperature of the inside members is mostly experiencing the almost same temperature as ambient temperature. The left and right-side truss members are showing some temperature variation through the time. In figure 4 (a), in the early part of the day the temperature in the upper deck is 39.7°C and the temperature of the rest of the bridge members is maintaining almost the same behavior.

**4.1 TEMPERATURE DISTRIBUTION OF STEEL ORTHOTROPIC HIGHWAY DECK DURING DAY TIME**

The temperature on the steel deck rises in a very rapid manner. In the early morning at 8 am, the temperature of the top surface is around 27.5°C, shown in figure 5(a). Within 4 hours it increases to 51.8°C at the outermost surface though the temperature at the bottom surface is still at 42.32°C which is about to rise. The temperature of the top sheet of the orthotropic girder is maximum at 3PM which is 59.8°C, in the meantime the lowest temperature in the bottom of the steel deck is around 55°C which is also significantly high. From this time of the day, the upper surface of the deck starts losing its temperature, on the contrary the bottom of the deck remains hot for few more hours and became cool in the night time. On the other hand, for the I shaped steel girder temperature change remains pretty consistent and depends on the upper steel deck. The bottom of this

steel girder maintains temperature around 29°C~31°C. And the upper side's temperature of this girder varies between 28°C to 54°C. Due to the small thickness and thermal properties of the steel member, temperature transmission through the girder to next steel member is significantly low, which means the consequences of rapid increment of temperature on deck have a very small effect on the other members next to the steel deck.

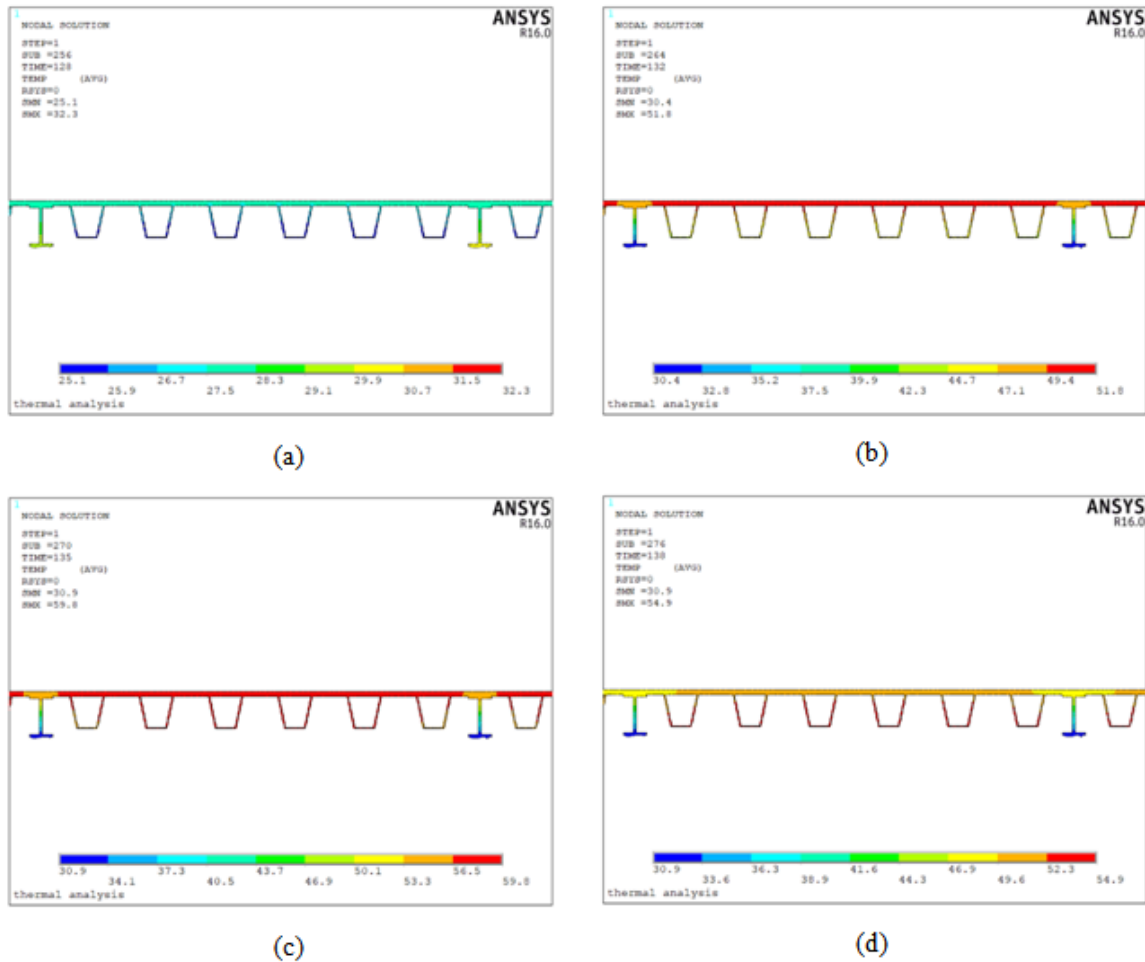


**Figure 5** Temperature distribution in the orthotropic deck (units: °C); (a) At 8 AM; (b) At 12 PM; (c) At 4 PM; (d) At 6 PM

**4.2 TIME-TEMPERATURE RELATIONSHIP OF STEEL DECK**

Two key points have been selected in the orthotropic bridge deck (figure 6) to show out the temperature-time curve, which has been shown in figure 7.

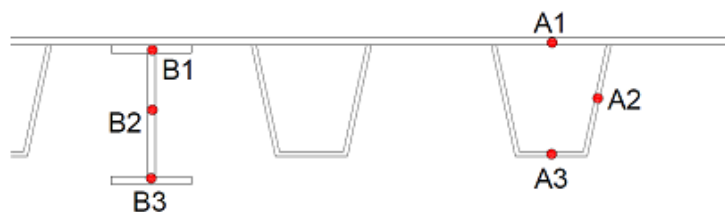


**Figure 6** Key points in orthotropic deck

The time-temperature curve for different key points in the orthotropic deck is significantly similar due to the very small thickness of the steel deck. Temperature rise and fall throughout the 24 hours of a day is  $37^{\circ}\text{C}$  for the orthotropic deck which can be checked from figure 7 (a). The maximum temperature in the time of the day is around 3PM. From figure 7 (b) temperature change behavior of the steel girder can be checked on. The top of the girder has rapid temperature change salutation but at the bottom of the section temperature rise and fall are steady. The maximum temperature rise for the girder in a day is  $31^{\circ}\text{C}$ .

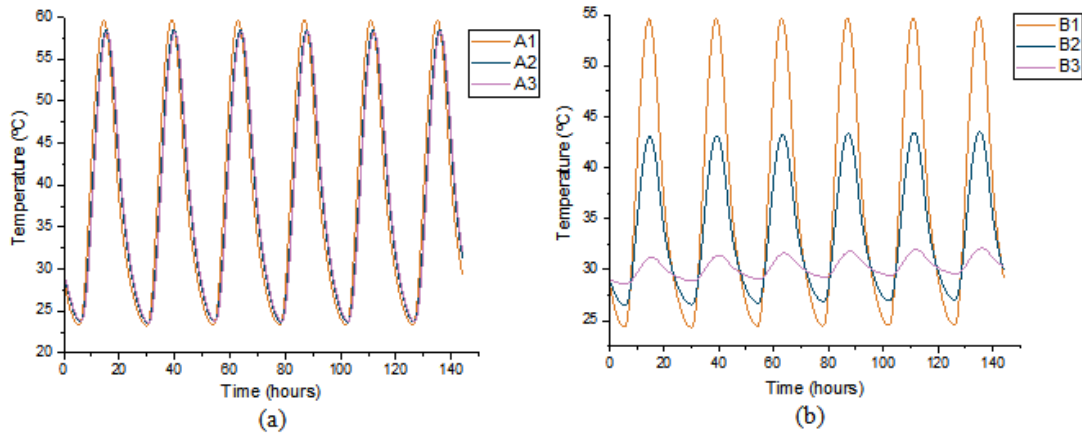


Figure 7 Time-temperature curve: (a) Point A; (b) Point B

#### 4.4 TEMPERATURE VARIATION THROUGHOUT THE DEPTH U-RIB SECTION

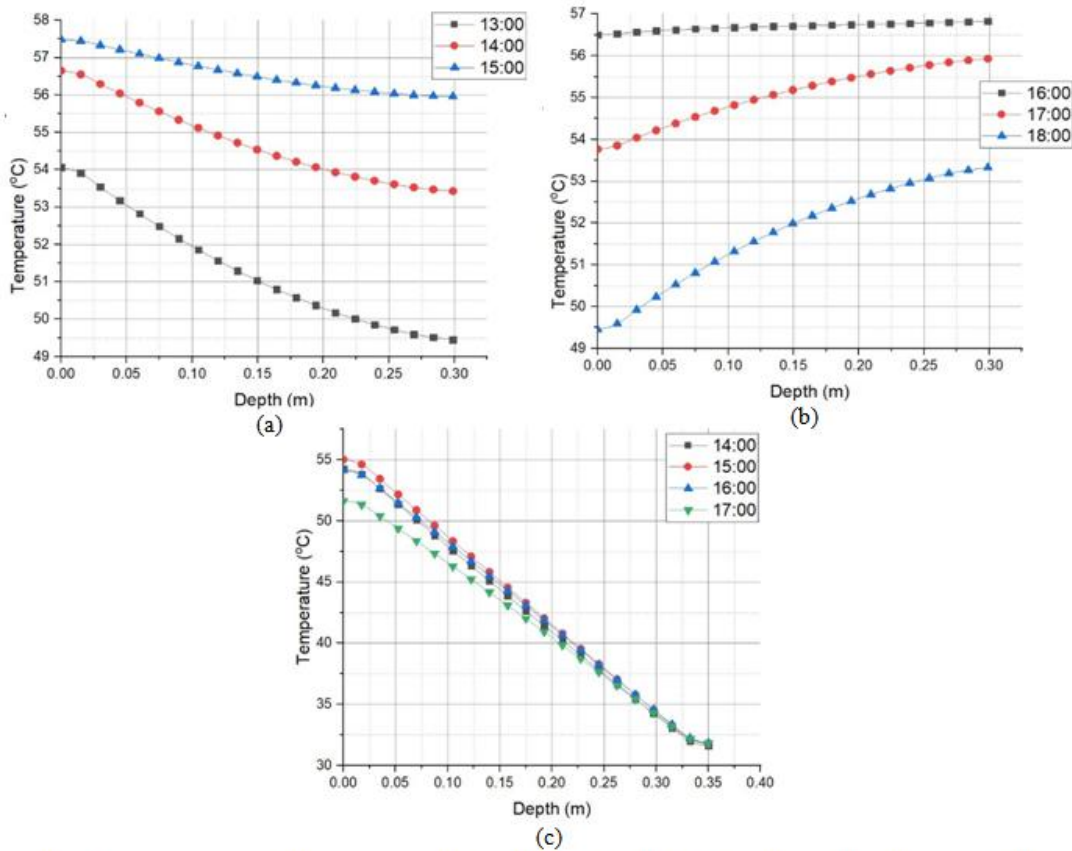


Figure 8 Temperature-depth curve: (a), (b) Depth throughout the U-rib section of the orthotropic deck; (c) "I" shaped steel girder

From figure 8 (a), it is clear that the temperature is changing linearly throughout the depth of the u-rip section of the orthotropic steel deck. In this figure the temperature has been shown from 1PM to 3PM. In this period of the day temperature of the top surface increases due to the sunlight. In this period the maximum temperature gradient is +5 °C. But the latter part of the day temperature of the upper surface starts decreasing and the remaining part of the deck remains hotter than the top surface. Which caused a negative temperature gradient for the deck, which can be checked from figure 8 (b). In these periods temperature gradient is roughly - 4 °C.

**4.5 TIME-TEMPERATURE RELATIONSHIP OF STEEL MEMBERS**

From the above analysis it seems that the temperature change inside steel members has less variation and maintains mainly the ambient temperature. And the outermost steel members, which experience solar radiation, are affected by temperature change. In figure 9(a) and 9(b), the time-temperature relationship of left side steel truss member and right-side steel truss member has been represented. It appears that for both members temperature is a sinusoidal curve. And the achieving time for maximum temperature varies due to their exposure to direct sunlight at a different time of the day. The daily temperature change in these members is roughly around 4.5°C to 5.5°C.

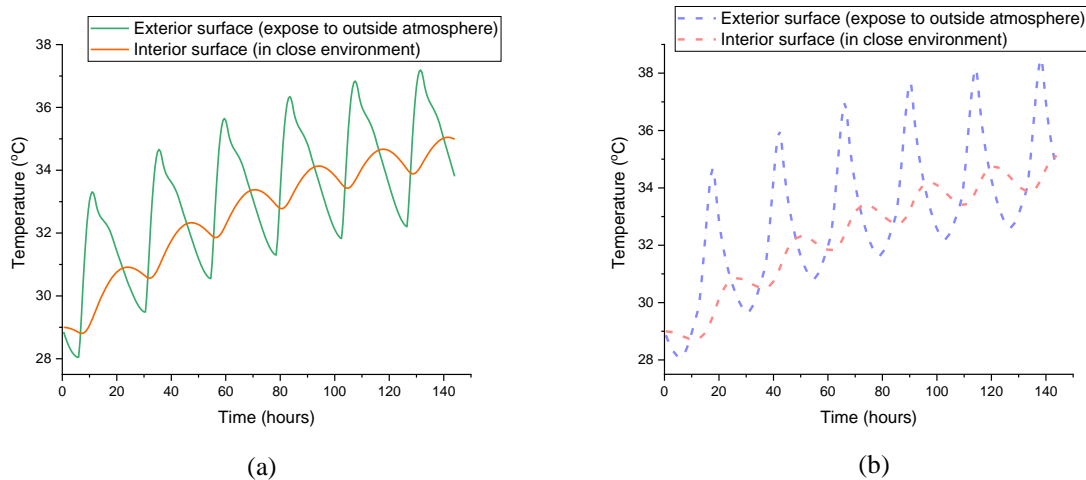


Figure 3 Time-temperature curve: (a)Left side steel truss member; (b) Right side steel truss member

**4.6 TEMPERATURE VARIATION THROUGHOUT THE DEPTH OF STEEL MEMBERS**

For the left side truss member, the maximum vertical temperature gradient is 3 °C at 12PM (figure- 10a) and for the right-side member this value is 3.2 °C at 4PM (figure- 10b) both are relatively low.

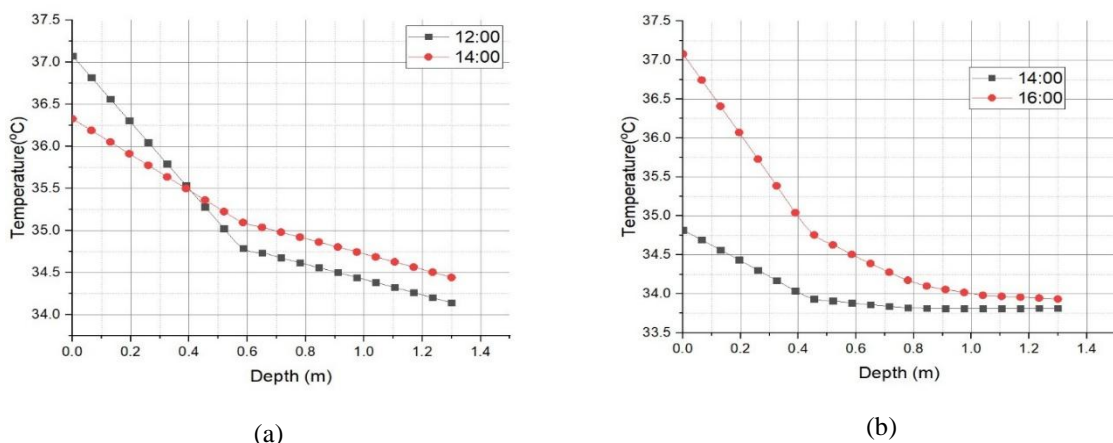


Figure 4 Time-depth curve: (a)Left side steel truss member; (b)Right side steel truss member

**V. THERMAL GRADIENT COMPARISON**

Due to different geographical locations and geographical features have an important impact on temperature distribution, different national bridge designs codes have differences in the specifications about temperature gradient in bridge superstructure. And most importantly in most of the national bridge codes have detailed code specifications about concrete bridges and some of them have guidelines about the steel-concrete composite bridge. But the specifications about steel bridges in national bridge design codes are limited. The British code is by far the most auspicious on temperature distribution load. In this study, the calculated thermal gradient is compared with British Code Specifications and German DIN101 specification.

**5.1 BRITISH CODE SPECIFICATIONS - BS5400<sup>[16]</sup>**

The temperature gradient values of bridges are divided according to the different types of the bridge superstructure. For steel deck with steel truss or steel girder (with specified thick of 40mm) bridge temperature gradient diagram has been shown in figure 11.

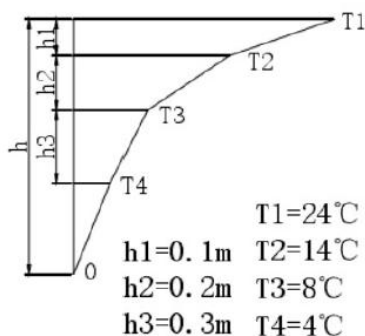


Figure 11 Temperature gradient diagram

**5.2 GERMAN DIN101 SPECIFICATION**

The vertical linear temperature difference values of different structure types have been represented in table 2.

**Table 2<sup>[17]</sup>: Vertical linear temperature gradient of different structure types**

Bridge super-structure type	Positive Temperature gradient (°C)	Negative Temperature Gradient (°C)
Steel Structure	18	-13
Steel concrete composite structure	15	-18
Concrete structure		
Concrete Slab	10	-5
Plate girder	15	-8
Precast slab	15	-8

The temperature difference values in Table 2 are measured for highway and railway bridges with 50 mm thick overlayer, and other thicknesses shall be multiplied by corresponding correction factors (see Table 3).

**Table 3<sup>[17]</sup>: Correction coefficient of temperature difference of pavement section with different thickness**

	Thickness of overlayer						
	0	50	80	100	150	300	Ballast bed (600)
Upper surface	1.5	1	0.82	0.7	0.5	0.3	0.6
Lower surface	1	1	1	1	1	1	1

**5.3 COMPARISON**

In bridge design code specifications, temperature represents in the form of a thermal gradient. To compare with these codes, the temperature gradient of the bridge throughout the bridge depth from 9 AM to 9 PM represents in figure 12. The temperature change in steel truss member is very small, so the temperature gradient of the top 1m of the bridge is shown this figure and the value of the thermal gradient after 0.8m tends to zero. The maximum thermal gradient is 25.2 °C at 3 PM. The temperature gradient (at 3 PM) comparison with BS5400 and DIN101 is shown in figure 13.

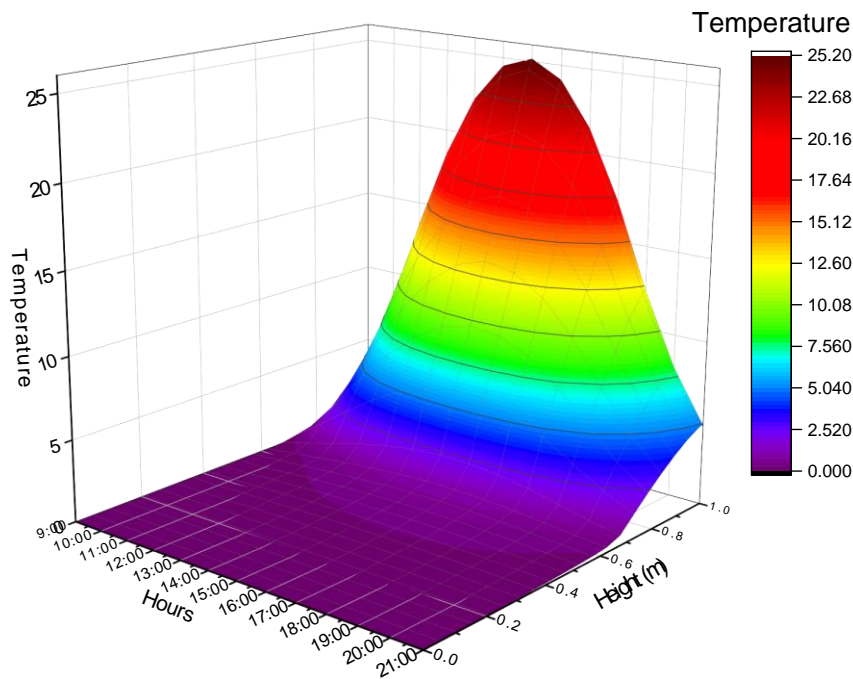


Figure 12 Thermal gradient diagram

The maximum thermal gradient in this study is 25.2°C which is lower than the DIN101 code (27°C) and slightly higher than the BS5400 (24°C). The climate in Wuhan, China is hotter in summer than both England and Germany so this maximum positive temperature gradient is considerable. Though long-term temperature analysis is required to get a more accurate result of the thermal gradient.

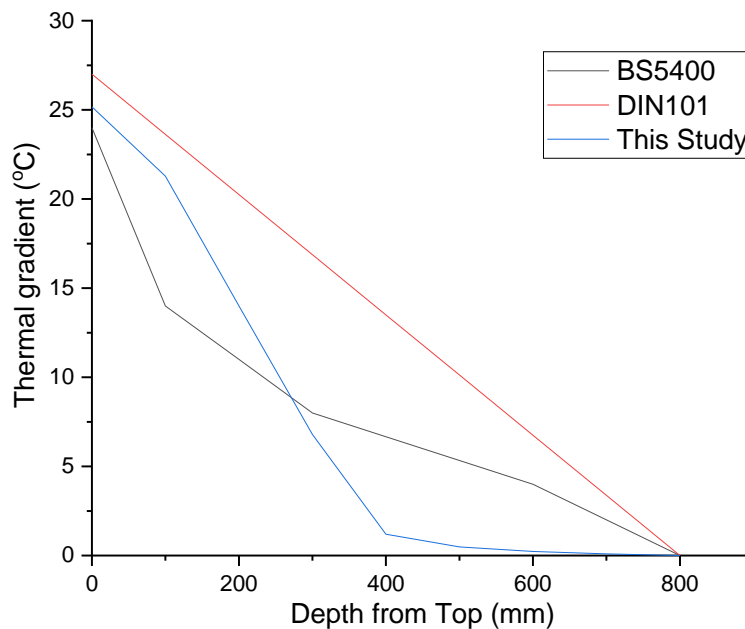


Figure 13 Thermal gradient comparison

### VI. CONCLUSIONS

The temperature distribution behavior of the orthotropic steel deck and steel truss frame in a steel truss bridge is investigated using ANSYS APDL software in this study. The findings of the study can be summarized as below:

- A numerical finite element model is introduced in this study which can be used with publicly available metrological data and sectional property of the superstructure. The calculated results of thermal gradient compared with two national bridge design code and the outcome confirms the reliability and feasibility of the method. So, it can be recommended that, this two-dimensional mathematical model can be directly used to temperature analysis.
- The maximum positive thermal gradient of the bridge is 25.2°C which is in the top of the bridge deck surface due to its exposure to direct solar radiation. So, the maximum thermal gradient for steel bridge superstructure under local environmental conditions of Wuhan, China can be considered (not less than) as 26°C.
- Due to the small thickness of the steel truss members and high thermal conductivity material property of steel, the temperature change throughout the thickness of these steel members is very small, the maximum temperature gradient is 3°C, which is negligible. The temperature change in the vertical depth of the steel truss member is also relatively very low which maximum value is 3.2°C.
- The maximum temperature in the upper surface of the highway orthotropic steel deck can be high as 59.8°C which is also justified by Cao et al <sup>[18]</sup> (61°C in The Zhanjiang Bay Bridge). This should consider in time of using any topping above the orthotropic steel deck.

### REFERENCES

- [1]. Wei C, Yi-ning L, Fang W.: Analysis of temperature difference effect of Long-Span Plate-Truss Composite Girder. *Bridge Construction* 49(2), 41-46 (2019).
- [2]. Zuk W.: Thermal behavior of composite bridges-insulated and uninsulated. *Highway Research Record* 76, 231-253 (1965).
- [3]. Emerson M.: The calculation of the distribution of temperature in bridges. TRRL Report LR 561, Department of the Environment, (1973).
- [4]. Potgieter C, William L G.: Nonlinear temperature distributions in bridges at different locations in the United State. *PCI Journal* 34(4), 81-103 (1989).
- [5]. Hirst M J S, Dilger W H.: Prediction of Bridge Temperatures. ETH Honggerberg, Zurich, Switzerland, IABSE Peridica 109-120 (1989).
- [6]. Tong M, Tham L. G, Au F T K, Lee P K K.: Numerical modelling for temperature distribution in steel bridges. *Computers & Structures* 79(6), 583-593 (2001).
- [7]. Backer H, Outtier A, Bogaert P.: Numerical and experimental assessment of thermal stresses in steel box girders. in *Proceedings of the 11th Nordic Steel Construction Conference (NSCC '09)*, 65-72 (2009).
- [8]. Ding Y, Zhou G, Li A, Wang G.: Thermal field characteristic analysis of steel box girder based on long-term measurement data. *International Journal of Steel Structures* 12(2), 219-232 (2012).
- [9]. Xia Y, Chen B, Zhou X., and Xu Y.: Field monitoring and numerical analysis of Tsing Ma suspension bridge temperature behavior. *Struct Contr Health Monit* 20(4): 560-75 (2013).
- [10]. KIM A S, PARK S, WU J.: Temperature variation in steel box girders of cable-stayed bridges during construction. *Journal of Constructional Steel Research* 112, 80-92 (2015).
- [11]. Liu, Y., Qian, Z., Hu, J., Jin, L.: Temperature Behavior and Stability Analysis of Orthotropic Steel Bridge Deck during Gussasphalt Pavement Paving. *Journal of Bridge Engineering*, 23 (1), art. no. 04017117 (2018).
- [12]. Liu K.: The Characteristics of Temperature Field on High Speed Railway Bridge Structure. Master Degree Thesis. Central South University, (2014).
- [13]. Pu Q, Liu J, Gou H, Bao Y and Xie H.: Finite element analysis of long-span rail-cum-road cable-stayed bridge subjected to ship collision. *Advances in Structural Engineering*, 1-13 (2019).
- [14]. Zheng P, Dai G.: A comparative study on static properties of a three-main-truss and three-cable-plane cable-stayed bridge. *Journal of Engineering, Design and Technology* 11, 207 - 220 (2013).
- [15]. <https://www.wolframalpha.com/input/?i=climate+in+wuhan> (accessed March 2020).
- [16]. BS5400 Steel concrete and composite bridge. part2: specification for loads. London: British Standards Institution; 1990.
- [17]. Deng S.: Large Span Steel Truss Girder Cable-stayed Bridge Temperature Effect Analysis. Master Degree Thesis. Changsha University of Science and Technology, (2014).
- [18]. Cao Y, Yim J., Zhao Y., and Wang M. L.: Temperature effects on cable stayed bridge using health monitoring system: a case study. *Structural Health Monitoring* 10(5), 523-537 (2011).

Pengfei Zheng, et. al. "Numerical Assessment of Temperature Distribution in the Orthotropic Steel Deck and Main Truss of a Rail-cum-road Bridge." *American Journal of Engineering Research (AJER)*, vol. 9(06), 2020, pp. 82-93.